

## Article

# Preparation and Characterization of Microencapsulated Ammonium Polyphosphate with Polyurethane Shell and Its Flame Retardance in Polypropylene

Thuy Tien Nguyen Thanh <sup>1</sup>, Ziya Yusifov <sup>1</sup>, Bence Tóth <sup>1</sup>, Katalin Bocz <sup>1</sup>, Péter Márton <sup>2</sup>, Zoltán Hórvölgyi <sup>2</sup>, György Marosi <sup>1</sup> and Beáta Szolnoki <sup>1,\*</sup>

<sup>1</sup> Department of Organic Chemistry and Technology, Faculty of Chemical Technology and Biotechnology, Budapest University of Technology and Economics, Műegyetem rkp. 3., H-1111 Budapest, Hungary; thuytien.nguyenthanh@edu.bme.hu (T.T.N.T.); bocz.katalin@vbk.bme.hu (K.B.); marosi.gyorgy@vbk.bme.hu (G.M.)

<sup>2</sup> Department of Physical Chemistry and Materials Science, Faculty of Chemical Technology and Biotechnology, Budapest University of Technology and Economics, Műegyetem rkp. 3., H-1111 Budapest, Hungary; marton.peter@vbk.bme.hu (P.M.); horvolgyi.zoltan@vbk.bme.hu (Z.H.)

\* Correspondence: szolnoki.beata@vbk.bme.hu

**Abstract:** Polypropylene (PP) shows no charring ability in burning due to the lack of hydroxyl functional groups; thus, the flame retardant system needs an additional amount of carbonizing agent. An ammonium polyphosphate (APP)-based all-in-one intumescent flame-retardant system was prepared by the in situ polymerization of polymeric methylene diphenyl diisocyanate (pMDI) with a glycerol-based and a glycerol-sorbitol-based polyol of high OH value. The microencapsulated APP with a polyurethane shell (MCAPP) of different polyols was characterized. The MCAPP with speculated improved flame retardant performance was selected for further evaluation in the PP matrix at different loadings by means of standard flammability tests.



**Citation:** Nguyen Thanh, T.T.; Yusifov, Z.; Tóth, B.; Bocz, K.; Márton, P.; Hórvölgyi, Z.; Marosi, G.; Szolnoki, B. Preparation and Characterization of Microencapsulated Ammonium Polyphosphate with Polyurethane Shell and Its Flame Retardance in Polypropylene. *Fire* **2024**, *7*, 97. <https://doi.org/10.3390/fire7030097>

Academic Editors: Yan Ding, Keqing Zhou and Kaili Gong

Received: 2 February 2024  
Revised: 1 March 2024  
Accepted: 13 March 2024  
Published: 19 March 2024



**Copyright:** © 2024 by the authors. Licensee MDPI, Basel, Switzerland. This article is an open access article distributed under the terms and conditions of the Creative Commons Attribution (CC BY) license (<https://creativecommons.org/licenses/by/4.0/>).

**Keywords:** flame retardancy; polypropylene; microencapsulation; ammonium polyphosphate; polyurethane shell

## 1. Introduction

Polypropylene (PP) is a thermoplastic polymer used for a broad array of applications in automobiles, medicine, construction, packaging, textiles, and furniture [1]. What makes this polymer advantageous over others is its rigidity, crystallinity, low density, chemical resistance, low cost, and processability [2]. However, PP has deficiencies, such as poor thermal stability and high flammability, that prevent its widespread use in electric and electronic applications [3]. Due to its entirely aliphatic hydrocarbon composition, PP burns swiftly, with a flame that produces little smoke and leaves no char behind [4]. Thus, the advancement of PP's thermal and flame-retardant properties is crucial. In the literature, many different types of flame retardants have been investigated and considered to improve the fire properties of PP, and one of the most current approaches is the application of novel microencapsulated ammonium polyphosphate (MCAPP). The microencapsulation of ammonium polyphosphate (APP) has the advantage of improving water resistance [5,6], increasing the interfacial compatibility between APP and the polymer matrix [7,8] and creating a complex formulation of an all-in-one intumescent flame-retardant system [9].

For the microencapsulation of APP, several common compounds such as epoxy resins, melamine-urea-formaldehyde, or cyclodextrin were researched for suitable shell materials [10]. Polyurethane (PU) is a promising shell material for microencapsulation as its polyol component has hydroxyl groups in its molecular structure so that it can be used as a charring agent in the flame-retardant system. Saihi et al. [11] contemplated that the combination of polyurethane and phosphate, in the PU shell-microencapsulated APP, has

intumescent system characteristics, and they considered it to be a potential novel flame retardant. The microencapsulated form of the polyurethane–phosphate system is beneficial for improving water resistance and preventing the migration of flame-retardant additive. Few studies have been conducted on PU shell-microencapsulated APP applications, and fewer have focused on their applications in the PP polymer for flame retardance. Ni et al. [6] prepared the PU shell from the in situ polymerization of toluene-2,4-diisocyanate (TDI) and pentaerythritol (PER) around APP particles and applied the microcapsules in PU. The flame retardancy results show that the char formed by the decomposition of APP and the PU shell is effective in postponing the catalytic degradation of PU and improving its flame-retardant properties. Microencapsulation was also beneficial in increasing the water resistance of the flame-retarded PU composite. The introduction of polyethylene glycol (PEG) into the in situ PU shell polymerization increased the microcapsules' charring ability [12].

APP was microencapsulated with PU resin by in situ polymerization with PER, TDI, Tween-80, and dibutyl tin dilaurate (DBTDL) and compared with neat APP as both were applied in PP/ethylene propylene diene rubber composites [13]. In TGA, the microcapsules possessed relatively higher thermal stability when the temperature was up to 600 °C, despite the initial decomposition temperature being lower than that of the untreated APP. The composites with microcapsules could not pass the UL94 test; however, they all suppressed the intense dripping of PP and achieved a good LOI. The microencapsulated form showed better performance than the neat form of APP, which is attributed to the PU shell acting as a carbonizing agent.

Zheng et al. prepared the PU shell through the polymerization of melamine (MEL) and PER with 4,4'-diphenylmethane diisocyanate (MDI) [14]. Through a molecular dynamics simulation, they showed that the microencapsulation improved the compatibility of the flame retardants, as the PP/PU and PU/APP interfaces have stronger interfacial compatibility and stability than the PP/APP interface due to the strong interaction between the PP molecular chain and the non-polar units on PU polymer chain, and the hydrogen bond between PU and APP. In another experiment, dipentaerythritol (DPER) was used along with MEL and MDI as constituent materials for the PU shell [15]. The use of DPER increased the charring ability of PP due to the abundance of hydroxyl groups in its formation. This led to a 32.1% LOI value at a 30% loading of microencapsulated flame retardant, and they could achieve a V-0 rating in UL-94 at only 20% loading.

Chen et al. observed the flame retardance of thermoplastic PU-microencapsulated APP incorporated in PP polymer [16]. The TGA results demonstrated that microencapsulation resulted in a high amount of residue for the composites, with 37.2% compared to 20.4% of the PP/APP sample. It was observed that the LOI value of composites increased as the content of the microcapsules in the polymer increased, up to 22.9% for the composite with 30% additive content. At the same loading of 30%, the result for a sample with neat APP was only 20.1%. Though all the polymer composites failed UL-94 tests, samples with PU-microencapsulated APP did not show any dripping that otherwise would expand the fire threat, leading to more dire consequences. In cone calorimetry (CC), the peak heat release rate (pHRR) decreased around four times from neat PP to PP with microcapsules at 30% content. In addition, there was an improvement in time to ignition (TTI), total heat release (THR), smoke emission rates, and final residue properties. When the effects of neat APP and MCAPP at the same additive composition are compared, it can be suggested that microencapsulation with PU had a slightly better impact on composites.

In this work, we attempted to microencapsulate ammonium polyphosphate with an in situ polymerized polyurethane shell from glycerol and glycerol–sorbitol-based polyols with different OH values and applied the prepared microcapsules in polypropylene to improve its flame retardancy. The microcapsules were loaded at different concentrations, and the flame retardant's performance was analyzed through standard flammability tests.

## 2. Materials and Methods

### 2.1. Materials

Polypropylene Innopol CS2-9000 was provided by Inno-Comp Kft. (Tiszaújváros, Hungary). Exolit® AP 422-type ammonium-polyphosphate was received from Clariant (MuttENZ, Switzerland). G-polyol and GS-polyol were received from MOL Nyrt. (Budapest, Hungary) as polyether polyols in the experimental phase, glycerol-based (OH value: 375) and glycerol-sorbitol-based (OH value: 455), respectively. Polymeric methylene diphenyl diisocyanate (pMDI) as ONGRONAT2100 and Triazinecat catalyst were provided by BorsodChem Zrt. (Gödöllő, Hungary). Toluene solvent was purchased from Merck (Darmstadt, Germany).

### 2.2. Methods

#### 2.2.1. Preparation of Flame-Retarded PP Composites

##### Kneading

The flame-retarded PP samples were prepared in a Brabender Plasti-Corder Lab-Station coupled with a W 50 EHT 3Z-type internal mixer chamber (Brabender GmbH & Co. KG, Duisburg, Germany). The temperature and the rotor speed were set to 180 °C and 50 1/min, respectively. The PP granules were melted first, then mixed with the flame-retardant additives. The mixture was mixed for a total of 5 min.

##### Molding

The kneaded materials were then hot-pressed using a Collin Teach-Line Platen Press 200E-type heated press (Dr. Collin GmbH, München, Germany) within a mold of  $100 \times 100 \times 4 \text{ mm}^3$  size at 180 °C. When the material was melted in the form, it was then pressed under 20 kN for 2 min, then under 50 kN for 3 min, and finally cooled to 50 °C under 50 kN. The LOI and UL-94 flammability test specimens were obtained by cutting the plates with a table saw.

#### 2.2.2. Characterizations

##### Fourier-transform infrared analysis

Infrared spectra ( $4000\text{--}400 \text{ cm}^{-1}$ ) of the microcapsules were recorded using a Bruker Tensor 37-type Fourier-transform infrared (FTIR) spectrometer (Bruker Corporation, Billerica, MA, USA) equipped with an ATR unit in attenuated total reflectance (ATR) mode ( $4000\text{--}600 \text{ cm}^{-1}$ ) with a resolution of  $4 \text{ cm}^{-1}$  and 16 scan accumulation.

##### Scanning electron microscopy

Scanning electron microscope (SEM) images of the additives, the fracture surface of specimens, and the char residue were taken with a JEOL 6380LVa (JEOL, Tokyo, Japan)-type apparatus in a high vacuum. The accelerating voltage was 10–15 keV. The samples were fixed by conductive double-sided carbon adhesive tape and sputtered with gold by a JEOL 1200 ion sputter (JEOL, Tokyo, Japan) to prevent charge build-up on the surface.

##### Thermogravimetric analysis

Thermogravimetric analysis (TGA) measurements were carried out using a TA Instruments Q5000 Apparatus (TA Instruments LLC, New Castle, NH, USA) under 25 mL/min nitrogen gas flow. Samples of about 5 mg for the flame retardants and 10 mg for the polymer composites were positioned in open platinum pans. The samples were heated from 25 °C to 800 °C with a 10 °C/min rate (the precision on the temperature measurements was  $\pm 1.5 \text{ °C}$  in the temperature range of 25–800 °C).

##### Wettability tests

The wetting properties of the particles were studied using two methods. The powders were sprinkled on a small drop of water on a microscope slide (EpreDia, Breda, The Netherlands), then covered by a covering glass slide for studying the possible aggregation and accumulation of the particles at the water–air interface by an optical microscope (Karl Zeiss, Jena, Germany) in transmission mode. For the contact angle measurements, the particles were suspended in toluene, then the dispersion was dropped onto microscope slides. After the evaporation of the toluene, advancing water contact angles were measured

with a KRÜSS DSA 30 device by placing a 10  $\mu\text{L}$  droplet of ultrapure water (purified by an Adrona Integrity + system) onto the surface of the resultant layer. The contact angles were measured immediately after the droplet formation, at 25 °C and in a humid environment (at least 80% relative humidity).

#### Water resistance test

The specimens were immersed in distilled water at 80 °C and kept at this temperature for 72 h, changing the water every 24 h. Then, the treated specimens were taken out and dried at 80 °C for 72 h. The mass loss percentages were measured from the initial weight of the untreated samples and the final weight of the dried samples.

#### UL94

Standard UL94 flammability tests were performed according to [17,18]; the specimen dimensions for the test were  $100 \times 10 \times 4 \text{ mm}^3$ .

#### Limiting Oxygen Index

The limiting oxygen index (LOI) was determined on specimens with  $100 \times 10 \times 4 \text{ mm}^3$  dimensions according to [19] standard using an apparatus made by Fire Testing Technology Ltd. (East Grinstead, West Sussex, UK).

#### Cone Calorimetry

Cone calorimetry (CC) tests were carried out with a TCC 918 Cone Calorimeter by NETZSCH Taurus Instruments according to [20]. The specimen dimensions for the test were  $100 \times 100 \times 4 \text{ mm}^3$ ; a constant heat flux of  $50 \text{ kW/m}^2$  was set. The following parameters were obtained: peak heat release rate (pHRR) and its time of occurrence (tpHRR), total heat release rate (THR), time to ignition (TTI), mass residue, smoke release rate (SRR), smoke production rate (SPR), maximum average rate of heat emission (MARHE), and average specimen mass loss rate over the period between 10% and 90% of the specimen mass loss occurred ( $\text{MLR}_{10-90}$ ).

#### Raman spectroscopy

Raman spectra were recorded with a LabRAM (Horiba Jobin Yvon, Longjumeau, France) instrument with a  $\lambda = 532 \text{ nm}$  Nd-YAG laser source (40 mW nominal laser power). A filter of 0.6 OD was used to decrease the excitation beam intensity, thus reducing the chance of sample degradation. LabSpec 6 software was applied for data collection and parameter optimization. The exposure time was 100 s per point. The collected spectra were truncated between 800 and  $2000 \text{ cm}^{-1}$  for spectral analysis. After the background correction and normalization of the spectra, they were deconvoluted with BWF and Lorentzian line pairs [21] for the G and D peaks, respectively, with the Origin program.

### 3. Results and Discussion

#### 3.1. Preparation of Microencapsulated Ammonium Polyphosphate

The microcapsules were prepared in a 4:1 mass ratio of APP to PU shell. The equivalent weights of polyols and pMDI for mixing the respective G-PU and GS-PU are listed in Table 1.

**Table 1.** Equivalent weights of polyols and ONGRONAT2100 for G-PU and GS-PU.

PU Formulation	G-Polyol [g/eq]	GS-Polyol [g/eq]	pMDI [g/eq]
G-PU	1.1	-	1
GS-PU	-	0.9	1

The APP and the polyol component were oven-dried at 80 °C before the synthesis. The APP, the polyol, and the pMDI were washed in a round-bottomed flask with toluene (7 mL toluene/1 g APP) and a few drops of catalyst were added. Then, the mixture was continuously stirred and kept for 4 h at reflux temperature (111 °C). After the heating was turned off, the stirring continued for a total of 24 h, counting from the mixture reaching the reflux temperature. Then, the mixture was filtered, and the separated microcapsules were dried at 80 °C overnight. The dried microcapsules were powdered in a hand mortar to obtain the microencapsulated flame retardants.

The yield is the percentage of the final mass of the filtered and dried product divided by the total mass of the initial reagents (APP, polyol, and pMDI). The average yield for G-polyol-based microcapsules was 47% while for GS-polyol-based microcapsules, it was 70%. Under the same conditions, the microencapsulation with GS-polyol gave 1.5 times higher yield on average than the one with G-polyol. The higher OH value of GS-polyol is assumed to be more beneficial to promote the in situ polymerization of the PU shell. The success of the microencapsulation was confirmed with further analyses.

### 3.2. Characterization of Polyurethane Shell Microencapsulated Ammonium Polyphosphate

The presence of the PU shell was first confirmed with Fourier-transform infrared analysis (FTIR). The most prominent peaks on the spectra of G-MCAPP and GS-MCAPP microcapsules were the characteristic absorption peaks of neat APP as expected since APP comprises about 80% of the microcapsules. Meanwhile, the polyurethane-specific bands for the G-PU and GS-PU components were also detectable as indisputable evidence of the successful microencapsulation.

In Figure 1, the specific peaks for the PU shell, such as CH<sub>2</sub> stretching at 2985 cm<sup>-1</sup>, C=O nonbonded urethane and C=O-associated urethane stretching without hydrogen at 1720 cm<sup>-1</sup>, H-N-C=O amide II combined motion at 1526 cm<sup>-1</sup>, N-H deformation vibration and C-N stretching vibration combined at 1230 cm<sup>-1</sup>, and C-O-C symmetric and asymmetric vibration at 1100 cm<sup>-1</sup>, can be seen for both microcapsules, evidencing their successful formation.

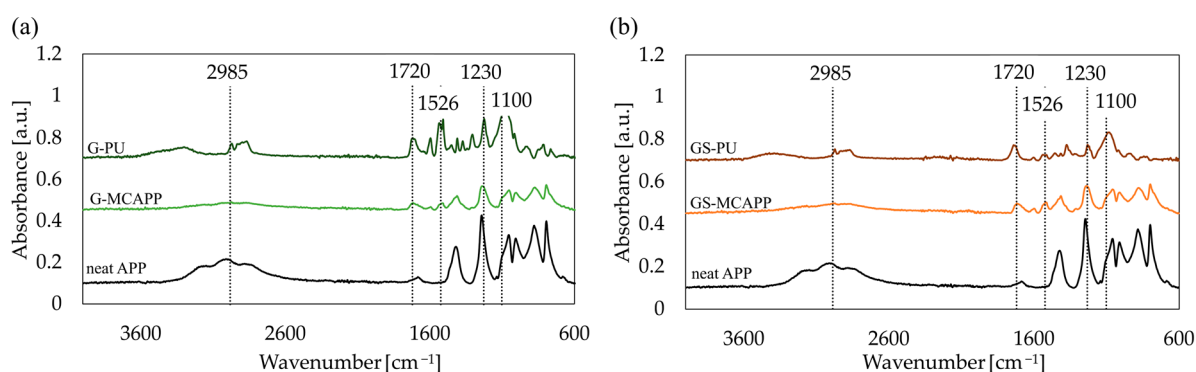


**Figure 1.** FT-IR spectra of neat components and the microcapsules; (a) G-MCAPP, (b) GS-MCAPP.

Under the scanning electron microscope (SEM), both G-MCAPP and GS-MCAPP show the presence of the shell layer compared to the neat APP, as seen in Figure 2. G-MCAPP microcapsules have rough textures, and tears of the shell are visible, even though this proves that the microencapsulation by G-PU was successfully achieved. Microencapsulation with GS-PU seems to be more advantageous since the GS-MCAPPs have smoother and rounder surfaces, do not reveal any cracks or holes, and cover all the sharp edges of APP.

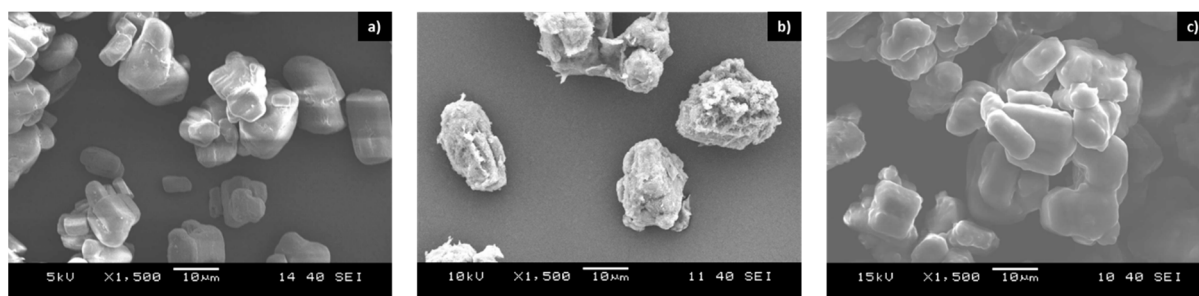


**Figure 2.** SEM images of (a) neat APP particles, (b) G-MCAPP, and (c) GS-MCAPP.

The thermal stability of microcapsules was analyzed with thermogravimetric analysis. The obtained decomposition curves of G-MCAPP and GS-MCAPP were compared to the

theoretical decomposition curves derived from their neat components' decomposition in TGA; the curves are shown in Figure 3. All the actual and theoretical decomposition curves show two degradation steps, but the first degradation step of the microcapsules started earlier, at a lower temperature than their respective theoretical curve, indicating the lowering effect of the PU shell on the thermostability of the flame retardant. However, the decomposition rate in the second step was slower and a much greater mass remained at 600 °C compared to the theoretical curves. This is attributed to the formation of the charred residue through the interaction of the PU shell and the APP core in the microcapsules.

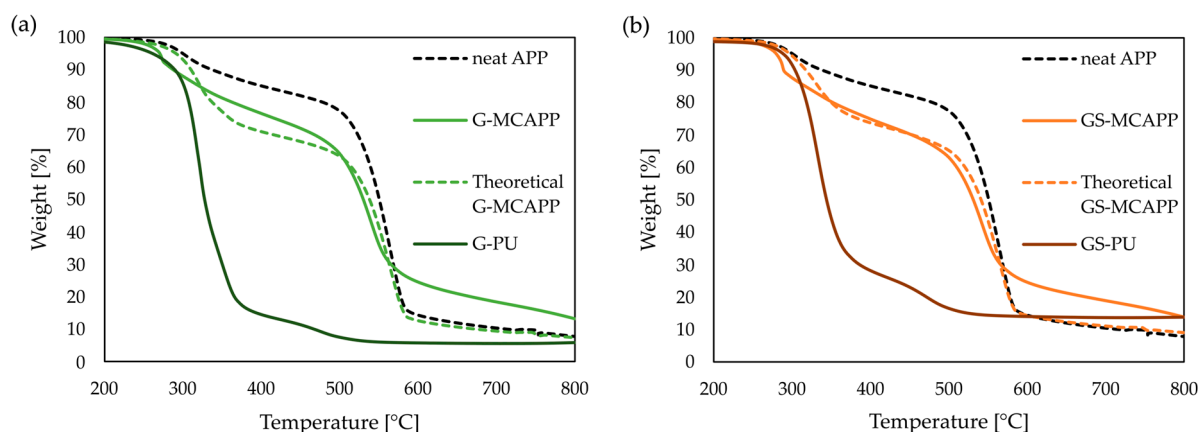


**Figure 3.** Decomposition curves of neat APP, its theoretical composition with (a) G-PU for G-MCAPP and (b) GS-PU for GS-MCAPP, respectively, in  $N_2$  atmosphere.

Both microcapsule formulations show very similar decomposition behaviors to each other, but the GS-MCAPP demonstrates slightly better thermostability than the G-MCAPP as the decomposition started 9 °C higher, had a slower maximum decomposition rate, and a higher mass residue left at 800 °C (Table 2).

**Table 2.** TGA results of the G-MCAPP and GS-MCAPP microcapsules and neat APP, in  $N_2$  atmosphere.

Sample	$T_{5\%}$ [°C]	$T_{50\%}$ [°C]	$dT_{max}$ [%/°C]	$T_{max}$ [°C]	Mass Residue [%]
neat APP	300.2	550.7	1.14	563.4	7.9
G-MCAPP	270.9	530.4	0.72	540.4	13.3
GS-MCAPP	279.7	531.0	0.70	542.8	13.9

The analyses on microcapsules confirmed the presence of the PU shell on both microcapsules with GS-MCAPP demonstrating better properties overall. In the preparation of flame-retarded polypropylene composites, only GS-MCAPP was used as flame retardant because the average yield was higher in its synthesis, its SEM image revealed a better structure of the microcapsules, and its decomposition temperature was closer to that of the neat PP. The GS-MCAPP microcapsules were added to the PP matrix at 15%, 20%, 25%, 30%, and 35% of the loading level.

The wetting properties of the neat APP and microencapsulated GS-MCAPP particles were investigated by optical microscopy and contact angle measurements. According to micrographs, the APP particles were dispersed in the water phase and uniformly located in the entire droplet. However, the GS-MCAPP particles formed aggregates and primarily grouped at the water–air interface, which suggests the hydrophobic character of the PU shell. The images of 10  $\mu$ L water droplets on the surface of the dried layers of the APP and GS-MCAPP particles are shown in Figure 4.

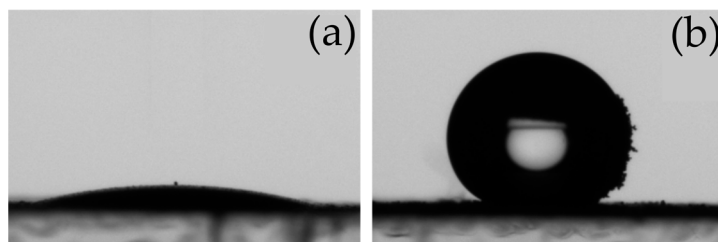


**Figure 4.** Images of water droplets on the dried layers consisting of (a) APP and (b) GS-MCAPP particles. In picture (b), the particles stuck to the right side of the droplet, trapped in the water–air interface revealing the partial wetting of GS-MCAPP particles.

As can be seen, the advancing water contact angle for the layer of the APP particles was under  $10^\circ$ , which highlights the hydrophilic character of the particles. In contrast, an advancing water contact angle of  $142 \pm 2^\circ$  could be measured on the layer formed from the GS-MCAPP particles that indicated the hydrophobic character of the PU shell. The surface of the layers formed by the drying of the suspensions can be rough, and the roughness can affect the measurable values of the contact angles (see, e.g., the Wenzel model [22,23]); however, the above measurements provide reliable information on the wettability: the PU shell renders the APP particles hydrophobic, which can improve the water resistance of the flame retardant.

### 3.3. Characterization of Flame-Retarded Polypropylene Composites

#### 3.3.1. Fracture Surface Analysis by Scanning Electron Microscopy (SEM)

The effect of microencapsulation on the dispersion and the interfacial interaction of particles within the PP matrix were analyzed by comparing the neat APP and the microencapsulated APP at the loading level of 20% under the SEM (Figure 5). The fracture surface of the PP/APP 20% sample shows partially detached particles and cavities left behind the fully detached particles, indicating weak interfacial interaction between the neat APP and the PP matrix. The composite containing the microcapsules in contrast have a less voided surface with particles embedded into the polymer. At this loading level of 20%, both particles show a similar degree of dispersion in the matrix. At higher loading levels of additives, the PP composites are assumed to have decreased mechanical properties as the presence of additives would increase the rigidity of the polymer and act as weak points in the structure. However, based on the above reported observations, the microencapsulation of APP could decrease the negative effect of the additives.

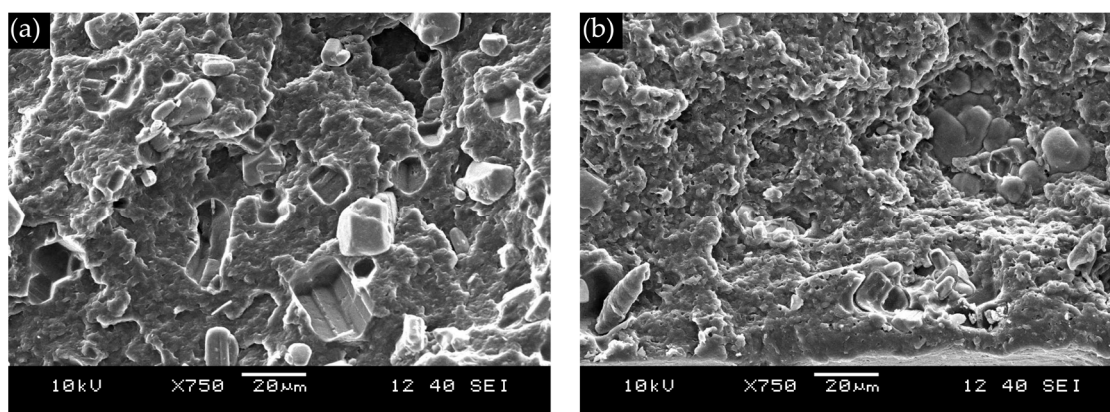


**Figure 5.** SEM images on the fracture surface of (a) PP/APP 20% and (b) PP/MCAPP 20% composites.

#### 3.3.2. Thermogravimetric Analysis (TGA)

The decomposition curves of the reference sample and the flame-retarded composites are shown in Figure 6. The thermal decomposition of neat PP started at a temperature

around 350 °C, higher than the flame-retarded composites, but it degraded completely in one step by 500 °C, leaving no mass residue. The addition of flame retardants shifted the decomposition temperatures to the lower temperature range; however, it significantly slowed down the decomposition rate as well. The composite samples degraded in several steps and yielded higher residual masses which are not attributable to the mass of added flame retardants in the composites, but rather to the beneficial interaction of the PU shell on the APP core in the microcapsules.

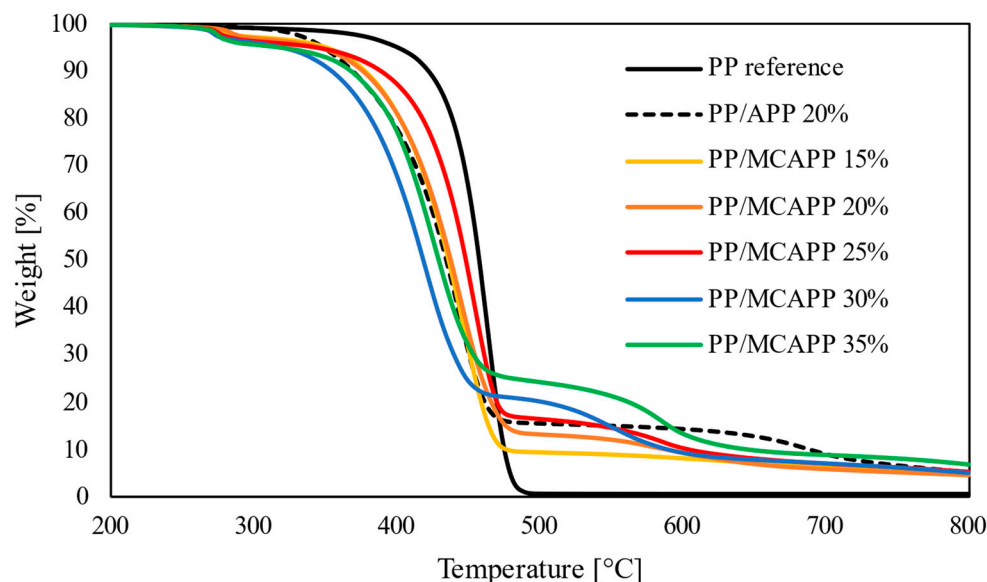


**Figure 6.** Decomposition curves of flame-retarded PP composites and reference sample in N<sub>2</sub> atmosphere.

In the case of composites with MCAPP, the higher the loading level of the flame retardant was, the earlier the decomposition of the samples started. The higher loading levels of microcapsules decreased the thermal stability of the composite; however, they seemed beneficial as the decomposition rate slowed and the residual mass increased for these samples, summarized in Table 3. In contrast, PP/APP 20% started to degrade earlier than the reference sample, but above 300 °C, while the first decomposition step of composites with microcapsules occurred below 300 °C. It was assumed to be from the degradation of the PU shell on the microcapsules, while the main step was assigned to the slower degradation of the PP matrix in the flame-retardant system.

**Table 3.** Results of TGA on flame-retarded PP composites and reference sample in N<sub>2</sub> atmosphere.

Sample Name	T <sub>5%</sub> [°C]	T <sub>50%</sub> [°C]	T <sub>max</sub> [°C]	dT <sub>max</sub> [%/°C]	Mass Residue [%]
PP reference	400.4	457.3	463.2	2.51	0.6
PP/APP 20%	348.4	434.4	442.9	1.28	5.2
PP/MCAPP 15%	350.5	436.1	446.7	1.38	4.7
PP/MCAPP 20%	345.2	437.5	445.2	1.23	4.5
PP/MCAPP 25%	343.3	448.1	453.9	1.59	5.3
PP/MCAPP 30%	319.4	418.3	419.4	1.08	5.0
PP/MCAPP 35%	317.7	429.0	425.9	1.08	6.8

The composites also had a third step above 450 °C, which became more prominent as the loading level increased, clearly visible for samples PP/MCAPP 30% and PP/MCAPP 35%. This step was assumed to be from the degradation of the charred remains formed by the interaction of the degrading PU and APP in the PP composites, which could not develop fully or at all at the lower loading levels and thus did not appear in the degradation

curves. PP/APP 20% has its second degradation step in this temperature region, assumed to be from the further decomposition of the mass that remained after the first step, but compared to the composites with microcapsules, this occurred at higher temperatures.

As the flame-retarded composites degraded earlier than the neat polymer and the composite with neat APP, a protective charred layer was formed, resulting in a lower decomposition rate and higher residual mass. The higher loading levels of the microcapsules proved to be beneficial, as the composite with the highest loading amount of 35% had the lowest decomposition rate and highest residual mass among all.

### 3.3.3. UL94 and LOI Flammability Tests

The effect of the microcapsules on the flammability of PP was studied first by small-scale flammability tests, such as UL94 and the limiting oxygen index (LOI). The neat PP sample obtained the lowest LOI value of 18 V/V% and the HB classification for UL94; the results are summarized in Table 4. The neat APP proved to be inefficient as it only increased the LOI by one unit. All composites with flame-retardant microcapsules showed improved LOI results: all samples obtained higher results than 21 V/V%. They achieved higher LOI values as their amount in the composites increased, proving the enhanced ignition resistance by the PU-microencapsulated APP in the PP polymer. The effect of the microencapsulation can be clearly seen comparing the LOI results of the 20% additive-containing samples. The use of neat APP led to a LOI value of 19 V/V%, while that of MCAPP resulted in 24 V/V%. This fact proves the synergistic effect of APP and the PU shell as reported in the literature [6,11]. In the UL94 test, most of the specimens could not pass the V-2 ratings. Zhou et al. [13] also reported that their microcapsules could not pass the UL94 test, while Zheng et al. [14] could achieve a V-0 rating at only 20% loading. When the amount of microcapsules reached 25%, the horizontal flaming stopped. The samples with 25 and 30% MCAPP fell back to the HB rating due to the long vertical burning times that exceeded the time limit for V-2 (250 s). The PP/MCAPP 35% sample reached a V-2 rating as it had significantly short burning times; however, the flaming droplets ignited the cotton.

**Table 4.** Results of UL94 and LOI tests on flame-retarded PP composites and the reference PP sample.

Sample Name	UL94	LOI [V/V%]
PP reference	HB (horizontal burning)	18
PP/APP 20%	HB (horizontal burning)	19
PP/MCAPP 15%	HB (horizontal burning)	23
PP/MCAPP 20%	HB (horizontal burning)	24
PP/MCAPP 25%	HB (burning time > V-2)	27
PP/MCAPP 30%	HB (burning time > V-2)	29
PP/MCAPP 35%	V-2 (ignition of cotton)	32

### 3.3.4. Water Resistance Test

Samples with a 20% additive content of neat APP and MCAPP in PP were water bath-treated and compared in the water resistance test. In the literature, microencapsulation was reported to improve the water resistance of the flame retardants (for example, by forming a hydrophobic barrier layer; see the end of Section 3.2); however, in our case, we observed a somewhat greater average mass loss in the PP/MCAPP 20% sample than in the PP/APP 20% sample (Figure 7). The treated specimens were then tested in the LOI, where we observed no change in the LOI values compared to the untreated specimens. The microcapsules with greater average mass loss were expected to decrease, but the fact that it remained unaffected showed that the composites with microcapsules were effective in retaining their flame retardancy after immersed in a water bath for 3 days.

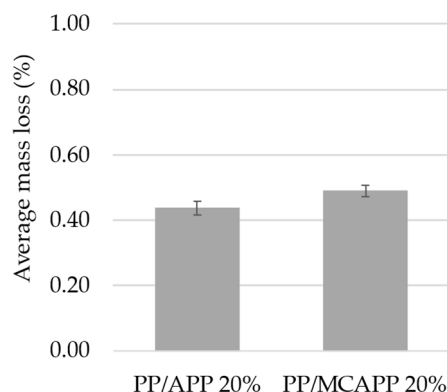


**Figure 7.** The average mass loss of the samples with 20% flame-retardant additive content after the water bath treatment.

After the water bath treatment, the fracture surface of the specimens near the edge was observed under the SEM (Figure 8). Some APP particles in the PP/APP 20% sample showed a disintegrated, broken surface, presumably hydrolyzed in the presence of water. In contrast, in the case of the microcapsule-incorporated composite, most of the particles were left intact. This demonstrated that the microencapsulation of APP with a PU shell can decrease the degree of disintegration when the composite is submerged in water for prolonged time.

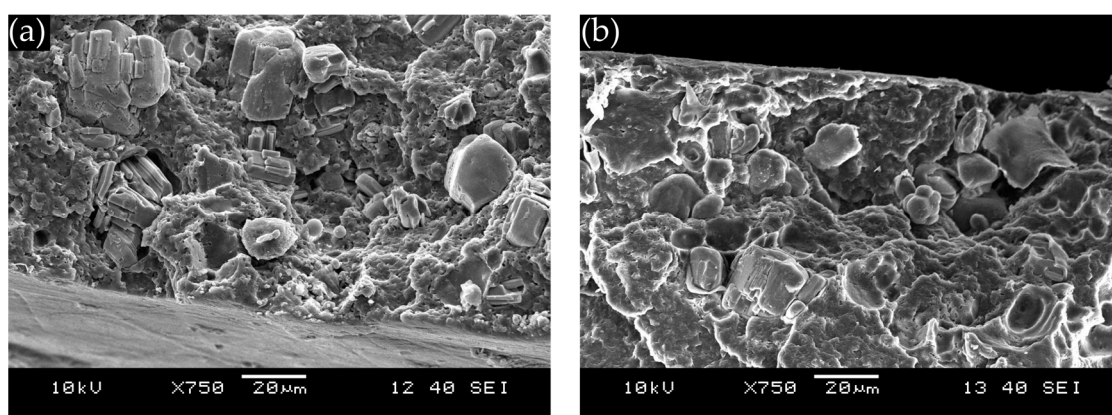


**Figure 8.** SEM images on the fracture surface of water bath-treated specimens of (a) PP/APP 20% and (b) PP/MCAPP 20% composites.

### 3.3.5. Cone Calorimetry

The effect of the microcapsules on the flammability of PP was further evaluated using cone calorimetry, an effective polymer fire behavior test characterized by long excessive heat exposure and the forced combustion of the flame-retarded samples.

The flame-retarded composites showed a suppressed heat release rate compared to the neat PP during combustion, as seen in Figure 9. The neat polymer burned immensely as it reached its peak heat release rate (pHRR) of 724 kW/m<sup>2</sup> in 212 s. The addition of neat APP could decrease the peak and delay its occurrence to some extent, but the addition of MCAPP showed more significant improvements, as in accordance with the LOI results. The time to ignition (TTI) showed a steady decrease up to the composite with the flame retardant content of 25%, then the trend reversed as the microcapsule content increased (see Table 5). In the TGA, the composites with the additive content of 15%, 20%, and 25% had their T<sub>5%</sub> within the range of 440–450 °C, while for the composites with 30% and 35% loads of microcapsules, it was considerably lower, around 420 °C (Table 3). It was speculated that the TTI correlates with the thermal stability of the composites; presumably during the ignition phase, the lower additive content is not sufficient to form an initial char

layer, while at the higher amount, the charring process is adequate to delay the ignition of the composite.

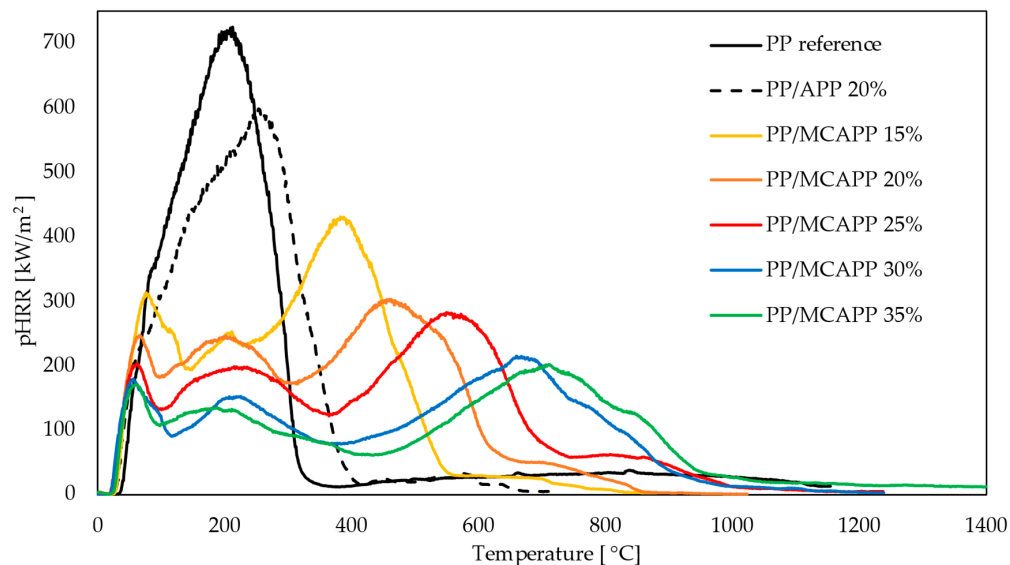


**Figure 9.** Heat release rates of flame-retarded PP composites and the PP reference sample under the heat flux of 50 kW/m<sup>2</sup>.

**Table 5.** Results of the CC test on flame-retarded PP composites and the reference PP sample under the heat flux of 50 kW/m<sup>2</sup>.

Sample	PP Reference	PP/ APP 20%	PP/ MCAPP 15%	PP/ MCAPP 20%	PP/ MCAPP 25%	PP/ MCAPP 30%	PP/ MCAPP 35%
TTI [s]	37	29	28	24	21	22	26
pHRR [kW/m <sup>2</sup> ]	724.9	598.1	430.6	302.6	282.1	214.4	201.3
tpHRR [s]	212	253	382	459	549	659	710
THR [MJ/m <sup>2</sup> ]	148.0	137.8	139.6	138.0	139.1	115.1	118.0
SRR [(m <sup>2</sup> /s)/m <sup>2</sup> ]	12.35	12.03	10.51	6.66	5.76	5.07	5.28
SPR [m <sup>2</sup> /s]	0.110	0.106	0.093	0.059	0.051	0.045	0.047
Mass Residue [%]	0.3	15.4	8.4	12.0	15.8	19.5	23.4
MARHE [kW/m <sup>2</sup> ]	426.9	375.2	264.7	214.9	180.5	129.4	119.1
MLR <sub>10-90</sub> [g/m <sup>2</sup> s]	4.65	5.21	4.33	3.68	2.95	2.76	2.17

As the MCAPP content in the polymer composites increased, the pHRR values decreased and shifted in time from 212 to 710 s at the maximum loading amount where the pHRR also decreased by approximately 73% compared to that of pure PP (Table 5). The total heat release (THR) values also decreased, while the mass residue increased with the incorporation of flame retardants and their increased content in the composite. These results are attributed to the sufficient char formation by the APP microcapsules with the PU shell. The higher loading level of MCAPP yielded stronger protective structures that acted as an effective heat barrier, which can be observed in the heat release curves, as they are distinctly flatter and prolonged in time.

The curves of neat PP and PP/APP 20% run steeply upwards as the thermal degradation of the materials released extensive heat due to the lack of the protective char layer, and the abrupt downward trend indicates the depletion of combustible material as the samples completely burned, leaving almost no residual mass in the case of the reference sample. The reason for the sharp rising and falling of the heat release curves is that the neat PP and PP/APP 20% composites did not contain any carbonizing agent that could help them create a protective charring layer to insulate the polymer from the fire. The samples

containing MCAPP showed typical intumescent-type curves [24] with an elongated heat release and peak value at the end of the burning.

Several peaks in the curves can be observed for microencapsulated flame retardant-containing composites. This showed that the formed char layer resisted while it was periodically damaged as the structural integrity of the char layer weakened, and after some time, it lost its protecting ability and finally exposed the remaining material to the heat source, resulting in the final peak hitting the maximum. However, these final peaks were much lower than the peak of the neat PP and PP/APP 20% sample, as less combustible material was left under the char layer at the final exposure. As the content of GS-MCAPP increased, the maximum of the peaks decreased, while the appearance of the second and third peaks shifted in time.

The efficiency of the formed protective char layer was further reflected in the  $MLR_{10-90}$  (average specimen mass loss rate over the period between 10% and 90% of the specimen mass loss occurred) values as it reduced by half in the case of the composite with the 35% loading level compared to the neat PP reference sample. Interestingly, the composite with neat APP had the highest  $MLR_{10-90}$  value that was speculated to be the result of the accelerated decomposition of the PP polymer by the acid catalysis of APP which otherwise would have affected the PU shell beneficially [25]. Higher flame retardant content showed a more suppressed smoke release, resulting in lower smoke release rate (SRR) and smoke production rate (SPR) values. The decreasing MARHE values indicated that the composites with higher flame-retarded content are less prone to spreading the flame to other objects.

When observing the char residues left after the combustion, noting that the neat PP burned completely without leaving any residue, the composite containing neat APP left a discontinuous layer of residue with small, seemingly charred bubbles with no significant height. When it was prepared for testing under the SEM, the consistency of the bubbles was sticky and gave the impression of pyrolytic products' residue (Figure 10a). The composites with microcapsules, on the contrary, had continuous, foamed, and charred residue, with heights varying from 1.5 cm to 2.0 cm as the content of the additive increased; for comparison, the photographs of PP/MCAPP 20% are shown in Figure 10b. These charred foams, however, lacked the compact, solid bulk structure as they showed a hollow internal cavity when cut across. For the SEM, the samples were prepared from the densest layer.

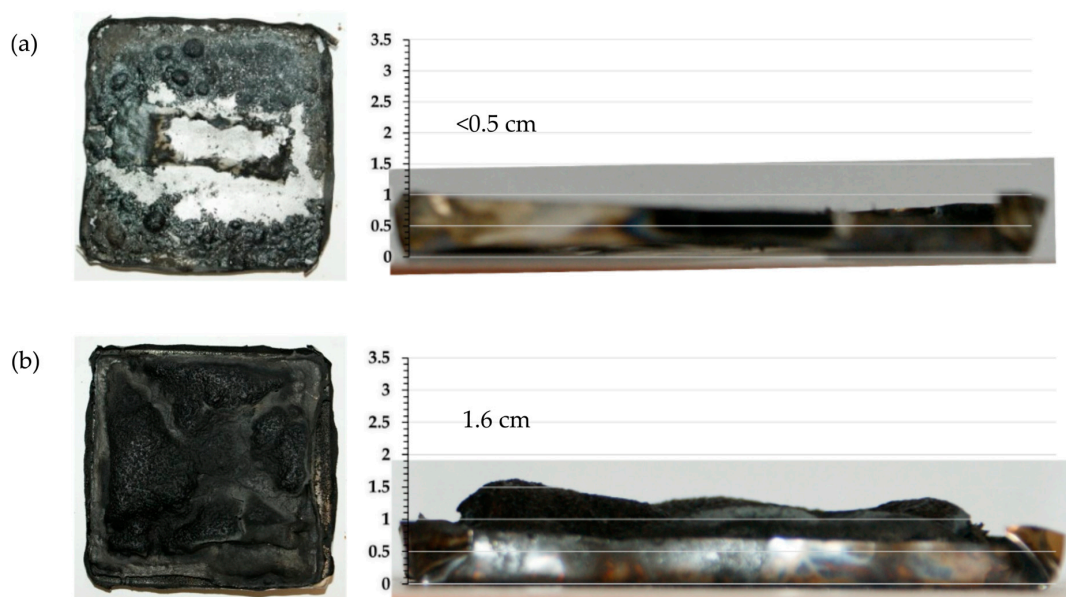


**Figure 10.** Photographs taken from above and from the side; (a) PP/APP 20% and (b) PP/MCAPP 20%.

The images taken using the SEM show the cross section of the charred layers at  $100\times$  and  $250\times$  magnification for PP/APP 20% and PP/MCAPP 20% (Figure 11). For the

composite with the neat APP, the cross section was a thin block with no holes or cavities, confirming our assumption that the bubbles consisted of degraded polymer and flame-retardant residue. The cross section of the composite with microcapsules showed a thicker inflated and bulging structure with holes of uneven size and distribution, evidencing the increased charring ability of the microcapsule-containing PP samples.

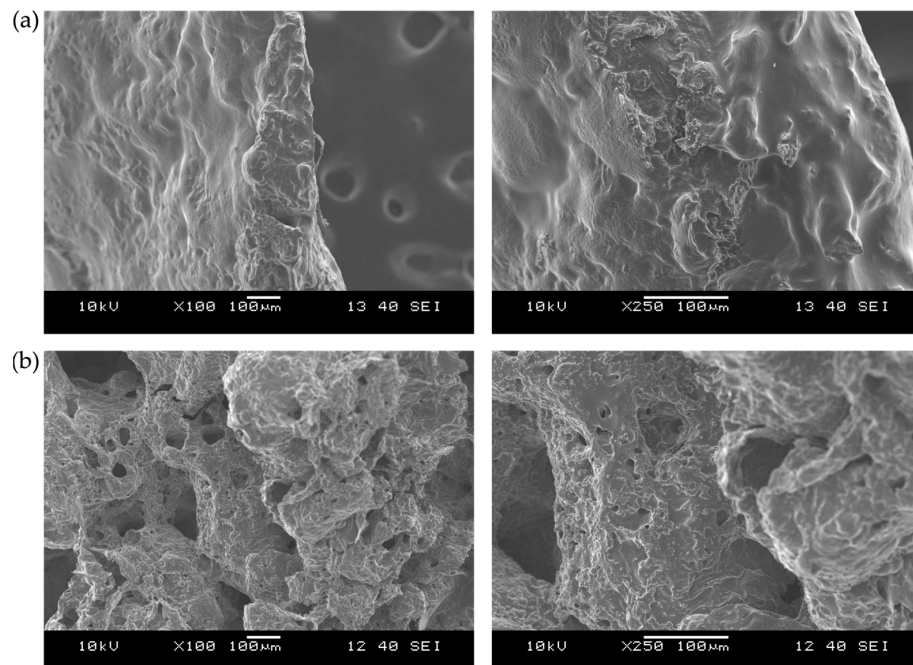


**Figure 11.** SEM images of the cross section of the flame-retarded composites' char residue at 100 $\times$  and 250 $\times$  magnifications; (a) PP/APP 20% and (b) PP/MCAPP 20%.

The charred residues of samples PP/APP 20%, PP/MCAPP 20%, and PP/MCAPP 35% were examined using Raman spectroscopy. The char residues have two distinct vibration bands near 1360  $\text{cm}^{-1}$  and 1580  $\text{cm}^{-1}$ , namely the D peak and G peak, respectively (Figure 12). The former is the mode of vibration of the carbon atom ( $\text{sp}^3$  hybridization), representing disordered carbonaceous structures, and the latter is the  $\text{E}_{2g}$  vibration of the C–C bond in graphite ( $\text{sp}^2$  hybridization), and the comparison between the intensities of these two bands is commonly used to indicate the degree of graphitization of the char layer.

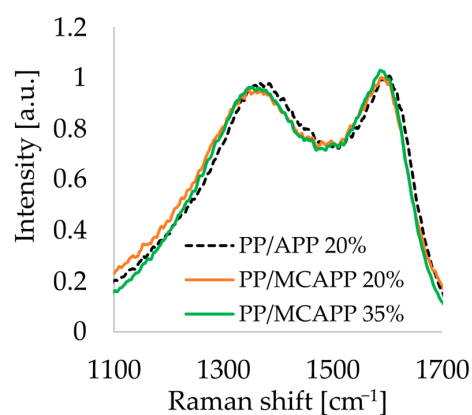


**Figure 12.** Raman spectra of the PP/APP 20%, PP/MCAPP 20%, and PP/MCAPP 35% composites' charred residue, normalized to the D band.

In Figure 12, the intensity ratios of the D and G peaks for the different samples seem to be similar to each other. Upon comparing their  $A_D/A_G$  ratios (listed in Table 6) that were

derived from the fitted D and G bands, the PP/APP 20% had the highest value, while for PP/MCAPP 20% and PP/MCAPP 35%, the ratios were lower. The lower  $A_D/A_G$  values signify a greater degree of graphitization and a denser char layer, so the microencapsulation of APP with the PU shell significantly improved the charring capabilities of the PP composites, and the higher additive amount showed a slightly greater degree of graphitization.

**Table 6.** Area ratios of the fitted D and G band of the char residues of PP/APP 20%, PP/MCAPP 20%, and PP/MCAPP 35%.

Sample	$A_D/A_G$
PP/APP 20%	2.73
PP/MCAPP 20%	2.61
PP/MCAPP 35%	2.57

#### 4. Conclusions

In this work, the preparation of microencapsulated ammonium polyphosphate was conducted using two different polyol components for the in situ preparation of the polyurethane shell. The glycerol–sorbitol-based polyol with a higher OH value proved to be a better candidate for the PU synthesis, as the yield was 1.5 times higher, as well as the morphological and thermal characteristics of the GS-MCAPP were better. In the water contact angle test, the PU shell was shown to impart hydrophobic properties to the APP particles, consequently enhancing the water resistance of the flame retardant. The microcapsules were used to prepare flame-retardant PP compositions. The thermal stability of the PP decreased to some extent with increasing MCAPP content, however the PU shell proved to be effective in decreasing the decomposition rate and the amount of the evolved degradation products compared to the neat APP. In LOI tests, the beneficial effect of the microencapsulation was evident: at the same additive content, the MCAPP sample reached 5 V/V% higher results. In cone calorimetry, the shape of the HRR curves of the MCAPP-containing samples showed a typical charring character, leading to gradually decreasing pHRR and THR values and increasing residual weight. The analysis of char residues using Raman spectroscopy concluded that microencapsulation could increase the degree of graphitization, while the SEM images on the cross section of the residues revealed a thicker inflated and bulging structure for the microcapsule-incorporated composites, evidencing their increased charring ability.

**Author Contributions:** Conceptualization, B.S. and K.B.; methodology, T.T.N.T., P.M., Z.H. and B.S.; validation, K.B., Z.H. and G.M.; investigation, Z.Y., B.T., P.M. and T.T.N.T.; resources, G.M., K.B., Z.H. and B.S.; writing—original draft preparation, T.T.N.T. and P.M.; writing—review and editing, B.S.; visualization, T.T.N.T., B.T., P.M. and Z.Y.; supervision, K.B., Z.H. and B.S.; project administration, K.B. and B.S.; funding acquisition, G.M., K.B. and B.S. All authors have read and agreed to the published version of the manuscript.

**Funding:** This research was supported by The National Research, Development, and Innovation Fund of Hungary under Grant TKP2021-NVA-02 and 2019–1.3.1-KK-2019–00004 projects. Support from the ÚNKP-23-5-BME-417 New National Excellence Program of the Ministry for Culture and Innovation from the source of the National Research, Development and Innovation Fund is acknowledged. B. Szolnoki acknowledges the financial support received through the János Bolyai Scholarship of the Hungarian Academy of Sciences.

**Institutional Review Board Statement:** Not applicable.

**Informed Consent Statement:** Not applicable.

**Data Availability Statement:** Data are presented within the article.

**Conflicts of Interest:** The authors declare no conflicts of interest.

## References

1. Younis, A.A. Flammability properties of polypropylene containing montmorillonite and some of silicon compounds. *Egypt. J. Pet.* **2017**, *26*, 1–7. [CrossRef]
2. Seidi, F.; Movahedifar, E.; Naderi, G.; Akbari, V.; Ducos, F.; Shamsi, R.; Vahabi, H.; Saeb, M.R. Flame Retardant Polypropylenes: A Review. *Polymers* **2020**, *12*, 1701. [CrossRef]
3. Vahabi, H.; Paran, S.M.R.; Shabaniyan, M.; Dumazert, L.; Sonnier, R.; Movahedifar, E.; Zarrintaj, P.; Saeb, M.R. Triple-faced polypropylene: Fire retardant, thermally stable, and antioxidative. *J. Vinyl Addit. Technol.* **2019**, *25*, 366–376. [CrossRef]
4. Hapuarachchi, T.D.; Peijs, T.; Bilotti, E. Thermal degradation and flammability behavior of polypropylene/clay/carbon nanotube composite systems. *Polym. Adv. Technol.* **2013**, *24*, 331–338. [CrossRef]
5. Zhang, Y.K.; Wu, K.; Zhang, K.; Wei, X.R.; Shen, M. Influence of Microencapsulation on Combustion Behavior and Thermal Degradation of Intumescent Flame-Retarded Epoxy Composite. *Polym.-Plast. Technol. Eng.* **2012**, *51*, 1054–1061. [CrossRef]
6. Ni, J.; Song, L.; Hu, Y.; Zhang, P.; Xing, W. Preparation and characterization of microencapsulated ammonium polyphosphate with polyurethane shell by in situ polymerization and its flame retardance in polyurethane. *Polym. Adv. Technol.* **2009**, *20*, 999–1005. Available online: <https://onlinelibrary.wiley.com/doi/full/10.1002/pat.1354> (accessed on 6 April 2020). [CrossRef]
7. Marosi, G.; Hirsch, E.; Bocz, K.; Toldy, A.; Szolnoki, B.; Bodzay, B.; Csontos, I.; Farkas, A.; Balogh, A.; Démuth, B.; et al. Pharmaceutical and Macromolecular Technologies in the Spirit of Industry 4.0. *Period. Polytech. Chem. Eng.* **2018**, *62*, 457–466. [CrossRef]
8. Wang, B.; Sheng, H.; Shi, Y.; Hu, W.; Hong, N.; Zeng, W.; Ge, H.; Yu, X.; Song, L.; Hu, Y. Recent advances for microencapsulation of flame retardant. *Polym. Degrad. Stab.* **2015**, *113*, 96–109. [CrossRef]
9. Nguyen Thanh, T.T.; Decsov, K.E.; Bocz, K.; Marosi, G.; Szolnoki, B. Development of Intumescent Flame Retardant for Polypropylene: Bio-epoxy Resin Microencapsulated Ammonium-polyphosphate. *Period. Polytech. Chem. Eng.* **2022**, *66*, 313–324. [CrossRef]
10. Lim, K.S.; Bee, S.T.; Sin, L.T.; Tee, T.T.; Ratnam, C.T.; Hui, D.; Rahmat, A.R. A review of application of ammonium polyphosphate as intumescent flame retardant in thermoplastic composites. *Compos. Part B Eng.* **2016**, *84*, 155–174. [CrossRef]
11. Saihi, D.; Vroman, I.; Giraud, S.; Bourbigot, S. Microencapsulation of ammonium phosphate with a polyurethane shell part I: Coacervation technique. *React. Funct. Polym.* **2005**, *64*, 127–138. [CrossRef]
12. Ni, J.; Tai, Q.; Lu, H.; Hu, Y.; Song, L. Microencapsulated ammonium polyphosphate with polyurethane shell: Preparation, characterization, and its flame retardance in polyurethane. *Polym. Adv. Technol.* **2010**, *21*, 392–400. [CrossRef]
13. Zhou, S.; Lu, H.; Song, L.; Wang, Z.; Hu, Y.; Ni, J.; Xing, W. Microencapsulated Ammonium Polyphosphate with Polyurethane Shell: Application to Flame Retarded Polypropylene/Ethylene-propylene Diene Terpolymer Blends. *J. Macromol. Sci. Part A* **2008**, *46*, 136–144. [CrossRef]
14. Zheng, Z.; Qiang, L.; Yang, T.; Wang, B.; Cui, X.; Wang, H. Preparation of microencapsulated ammonium polyphosphate with carbon source- and blowing agent-containing shell and its flame retardance in polypropylene. *J. Polym. Res.* **2014**, *21*, 443. [CrossRef]
15. Yu, S.; Xiao, S.; Zhao, Z.; Huo, X.; Wei, J. Microencapsulated ammonium polyphosphate by polyurethane with segment of dipentaerythritol and its application in flame retardant polypropylene. *Chin. J. Chem. Eng.* **2019**, *27*, 1735–1743. [CrossRef]
16. Chen, M.; Xu, Y.; Chen, X.; Ma, Y.; He, W.; Yu, J.; Zhang, Z. Thermal stability and combustion behavior of flame-retardant polypropylene with thermoplastic polyurethane-microencapsulated ammonium polyphosphate. *High Perform. Polym.* **2014**, *26*, 445–454. [CrossRef]
17. ISO 9772:2020; Cellular Plastics—Determination of Horizontal Burning Characteristics of Small Specimens Subjected to a Small Flame. International Organization for Standardization: Geneva, Switzerland, 2020.
18. ISO 9773:1998; Plastics—Determination of Burning Behaviour in thin Flexible Vertical Specimens in Contact with a Small-Flame Ignition Source. International Organization for Standardization: Geneva, Switzerland, 1998.
19. ISO 4589-2:2017; Plastics—Determination of Burning Behaviour by Oxygen Index Part 2: Ambient-Temperature Test. International Organization for Standardization: Geneva, Switzerland, 2017.
20. ISO 5660-1:2015; Reaction-to-Fire Tests—Heat Release, Smoke Production and Mass Loss Rate Part 1: Heat Release Rate (Cone Calorimeter Method) and Smoke Production Rate (Dynamic Measurement). International Organization for Standardization: Geneva, Switzerland, 2015.
21. Ferrari, A.; Robertson, J. Interpretation of Raman spectra of disordered and amorphous carbon. *Phys. Rev. B* **2000**, *61*, 14095. [CrossRef]
22. Yildirim Erbil, H. Dependency of Contact Angles on Three-Phase Contact Line: A Review. *Colloids Interfaces* **2021**, *5*, 8. [CrossRef]
23. Detrich, Á.; Nyári, M.; Volentiru, E.; Hórvölgyi, Z. Estimation of contact angle for hydrophobic silica nanoparticles in their hexagonally ordered layer. *Mater. Chem. Phys.* **2013**, *140*, 602–609. [CrossRef]
24. Scharrel, B. Phosphorus-based Flame Retardancy Mechanisms—Old Hat or a Starting Point for Future Development? *Materials* **2010**, *3*, 4710–4745. [CrossRef]
25. Grassie, N.; Mendoza, G.A.P. Thermal degradation of polyether-urethanes: Part 4—Effect of ammonium polyphosphate on the thermal degradation of polyether-urethanes prepared from methylene bis(4-phenylisocyanate) and low molecular weight poly(ethylene glycols). *Polym. Degrad. Stab.* **1985**, *11*, 145–166. [CrossRef]

**Disclaimer/Publisher's Note:** The statements, opinions and data contained in all publications are solely those of the individual author(s) and contributor(s) and not of MDPI and/or the editor(s). MDPI and/or the editor(s) disclaim responsibility for any injury to people or property resulting from any ideas, methods, instructions or products referred to in the content.